

Supporting information

Hollow polymer nanoparticles: Nature mimicking architecture for efficient hydrogen evolution

Aijie Liu^a, Cheuk-Wai Tai^b, Katerina Hola^a, Haining Tian^{a}*

^a Department of Chemistry-Ångström Lab., Uppsala University, Sweden.

^b Department of Materials and Environmental Chemistry, Arrhenius Laboratory, Stockholm University

*E-mail: haining.tian@kemi.uu.se

Table of Content:

- 1. Characterization of Pdots**
- 2. Characterization of Pdot-dye (HPTS) hybrid nanoparticles (NPs)**
 - 2a. Purification of Pdot-HTPS hybrid NPs.**
 - 2b. Physicochemical conditions of polymer vesicle**
 - 2c. Proton diffusion across polymer vesicles**
 - 2d. pH environment study under Photocatalysis process**
- 3. Effect of Pdots size and hollow structure on photocatalysis**
- 4. Hydrogen generation analysis with polymer organic droplet**

1. Characterization of Pdots

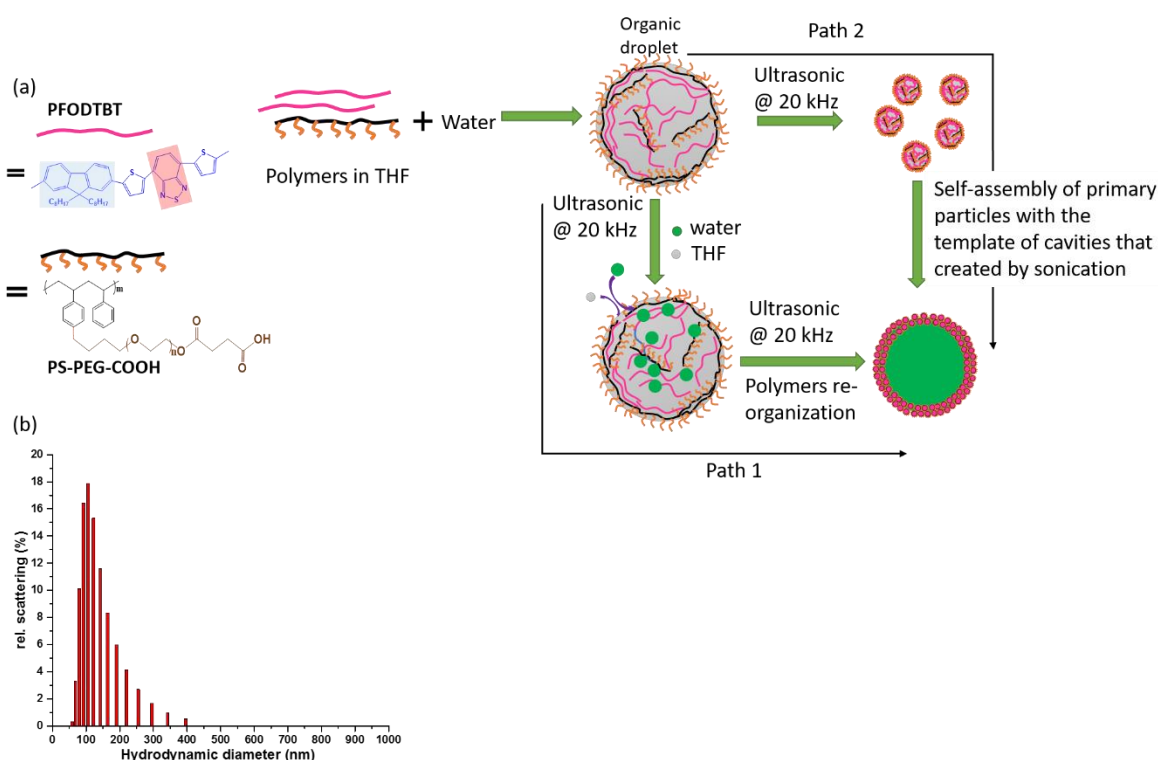


Figure S1. (a) Scheme of preparation of hollow polymer vesicles integrated with conducting polymer PFODTBT with amphiphilic polymer PEG-COOH grafted PS. (b) DLS analysis of polymer organic droplet dispersed in water before removing of THF, condition: water to THF = 2 : 1 vol/vol, PFODTBT concentration in THF phase: $50 \mu\text{g mL}^{-1}$.

Ultrasound assisted hollow nanoparticle preparation and the mechanism of hollow structure formation have been well studied elsewhere.¹⁻² There are two possible paths to form hollow polymer vesicles with porous shell, as shown in Figure S1a: 1) Polymer organic droplet dispersed in water first, with diameter of MN = 120 nm, as shown in Figure S1b. Under the assistance of sonication, water might replace THF phase in the droplets, with continuous THF evaporation, polymers re-organize into porous hollow nanostructures; 2) Polymer organic droplets split into small droplet under the assistance of sonication, primary particles were then formed after complete removal of THF through evaporation, finally these primary particles self-assembly into porous hollow nanoparticles with the assistance of sonication.

2. Characterization of Pdot-dye (HPTS) hybrid nanoparticles (NPs)

2a. Purification of Pdot-HPTS hybrid NPs.

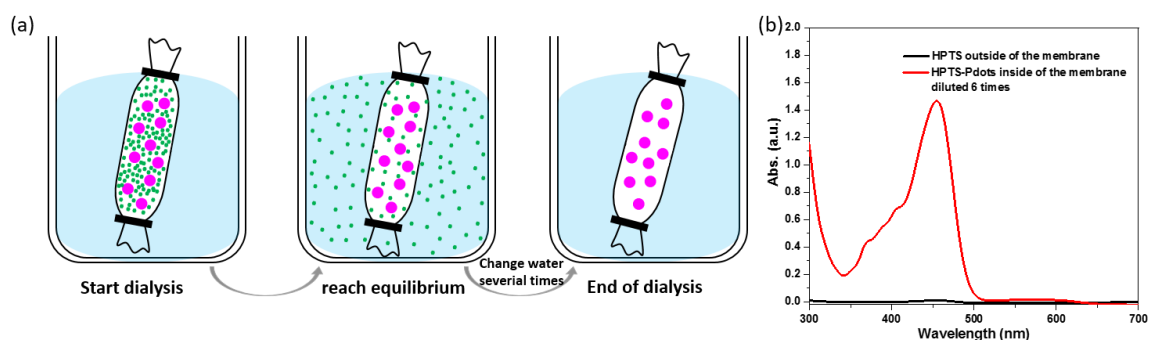


Figure S2. (a) scheme of dialysis procedure for HTPS encapsulated polymer vesicles (note as Pdot-HTPS) purification, green dots: free HTPS, purple dots: Pdot-HTPS; (b) UV-Vis analysis of purified Pdot-HTPS colloidal solution inside of dialyze membrane and solution outside of the dialyze membrane.

Purification of HTPS encapsulated polymer vesicles (note as Pdot-HTPS) were carried out by using dialyze membrane with MWCO 20 kDa, dialyze against pure deionized water for 2 days. Change water every 3 to 4 hrs until the amount of HTPS outside of the dialyzing membrane is negligible (as shown in Figure S2, less than 0.1 % of HTPS remained outside of the vesicle solution). HTPS are highly negatively charged and water soluble, therefore we can confirm that all encapsulated HTPS molecules should stay inside of polymer vesicles (instead of staying at the interface), however, it is hard to determine and specify whether molecules stay at the inner space of vesicle or stay close to the inner surface of vesicle shells. For either case, we demonstrate that it should not affect the result of proton diffusion in the following study. Again, in case of long-term storage (longer than a week), samples were purified again with dialyze cassette with MWCO 20 kDa before use.

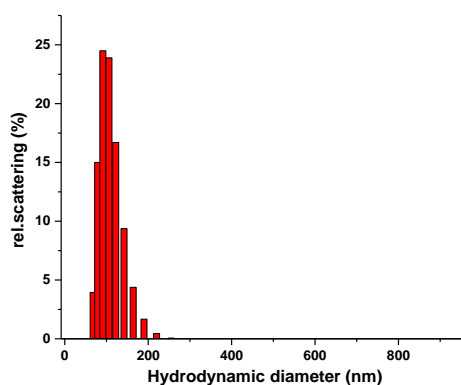


Figure S3. DLS analysis of Pdot-dye hybrid NPs.

2b. Physicochemical conditions of polymer vesicle

Internal pH determination

In order to determine the internal pH of vesicles, 8-hydroxypyrene-1,3,5-trisulfonic acid (HTPS) used as fluorimetric pH probe (see molecular structure at Figure S4, left image), since

it has been widely studied.³ HTPS is highly water soluble, has absorption maxima at $\lambda = 402$ nm and $\lambda = 455$ nm (shown in Figure S4, right image), with an emission maximum at $\lambda = 515$ nm.

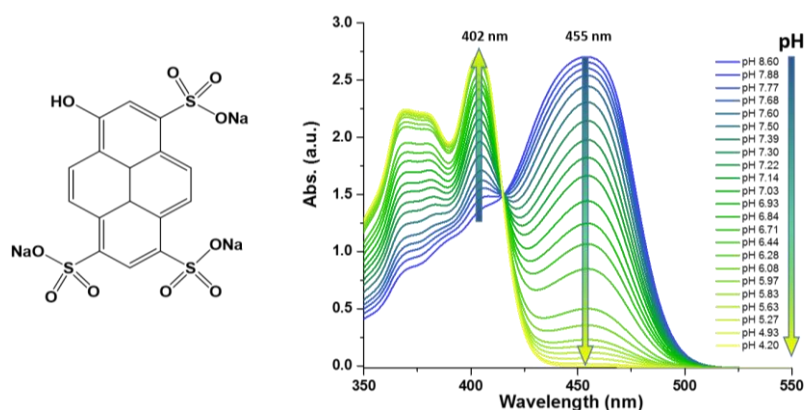


Figure S4. Fluorimetric pH probe HTPS molecular structure (left) and UV-Vis analysis of pH dependent absorption.

In order to study the pH environment in polymer vesicle under photocatalysis while avoiding effects from during reactions, such as hydrogen generation and diffusion, a model experiment was studied by using 0.2 M of acetic acid solution, same concentration of ascorbic acid used in photocatalysis process. Acetic acid shares similar pKa with ascorbic acid. Since photocatalytic reactions were all carried out around the optimal pH = 4 (bulk solution),⁴ pH environment in side of the polymer vesicle in the range of pH 4 to pH 5.5 was studied. Ratiometric measurements by taking ratio of fluorescence intensity at emission of $\lambda = 515$ nm with excitation at $\lambda = 455$ and $\lambda = 402$ nm.⁵ Measurements for free HTPS probe, Pdots nanoparticles with free THPS probe mixture (note as Pdots+dye mix) and Pdote-dye were all carried out at same HTPS concentration, raw data of emission with excitation at $\lambda = 455$ and $\lambda = 402$ nm are shown in Figure S5.

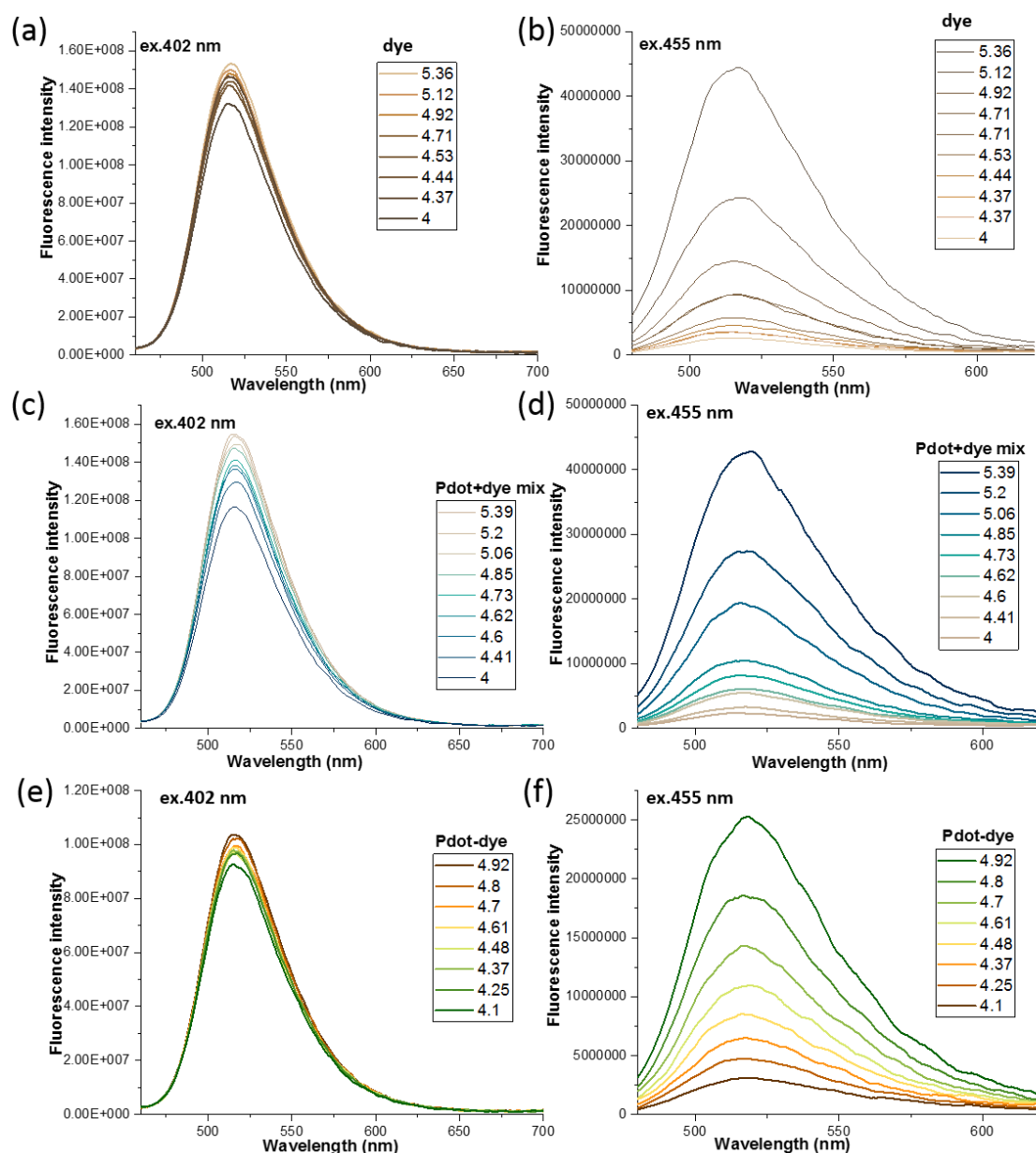


Figure S5. Raw data of maxima emission at $\lambda = 515$ nm with excitation of $\lambda = 455$ nm and $\lambda = 402$ nm of free dye, Pdot+dye mix and Pdot-dye hybrid NPs for pH determination of inside of polymer vesicles.

2c. Proton diffusion across polymer vesicles

In order to give a direct insight of fast proton diffusion across polymer membrane, maxima emissions at excitation of $\lambda_{\text{ex}} = 455$ nm and $\lambda_{\text{ex}} = 402$ nm were kinetically recorded for total 900 s (15 min), ratio of maxima emission at $\lambda_{\text{ex}} = 455$ nm and $\lambda_{\text{ex}} = 402$ nm were versus time were present in Figure S6. Both Pdot-dye and free dye were dispersed in 3 mL of 1 mM of phosphate buffer, with initial pH = 9.2, added 7 μL of 2 M of aqueous HCl solution at $t = 0$, final pH was measured with pH meter, pH = 6.90 and pH = 6.88 for Pdot-dye and free dye solution,

respectively. Kinetic emissions recorded for 900 s, 0.1 s per record. After then, another 3 μL of 2 M of aqueous HCl solution at $t = 0$, final pH was measured with pH meter, pH = 5.90 and pH = 6.10 for Pdot-dye and free dye solution, respectively. Again, kinetic emissions recorded for 900 s, 0.1 s per record. As shown in Figure S6, proton diffusion across polymer vesicle is fast in all pH range that we studied, which is too fast to study with technique we used here.

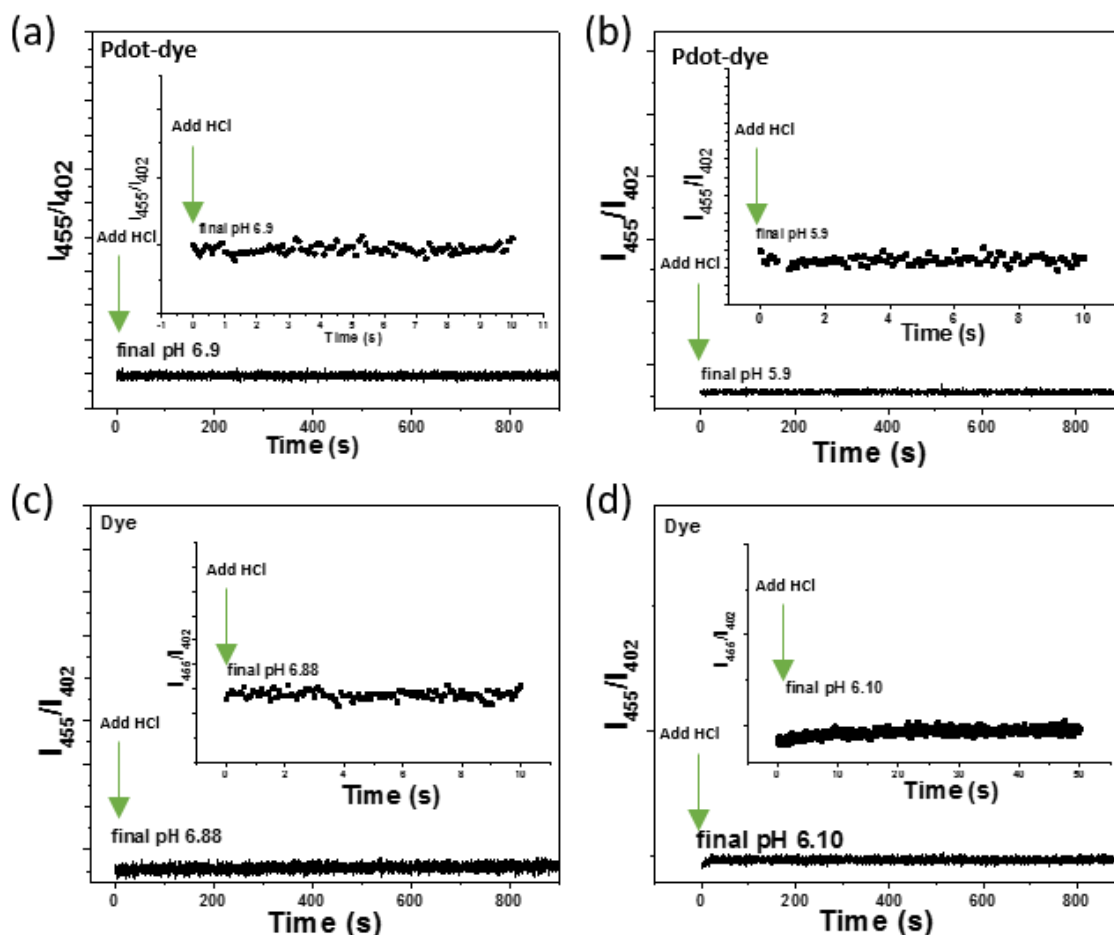


Figure S6. Kinetic monitoring of maximum emission at excitation of $\lambda = 455$ nm and $\lambda = 402$ nm, under experimental condition of 1 mM phosphate buffer, 3 mL in total. Add 7 μL of 2 M HCl at $t = 0$ for (a) and (c); add another 3 μL of 2 M HCl at $t = 0$ for (b) and (d).

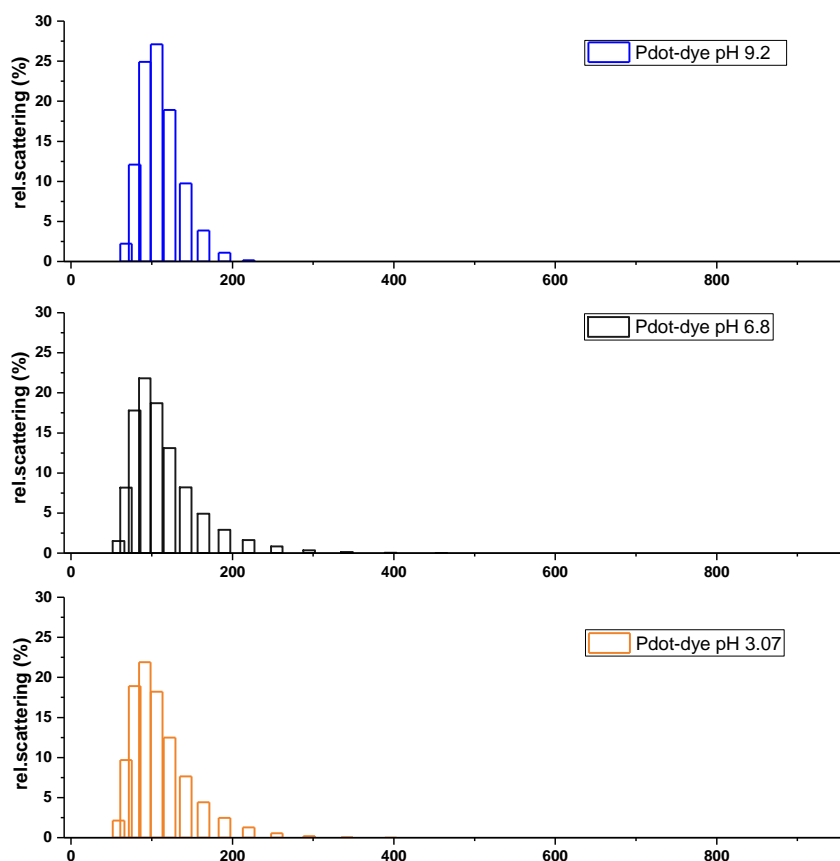


Figure S7. DLS analysis of Pdot-dye hybrid system under acidic pH 3.07, near neutral pH 6.8 and base pH 9.2;

DLS analysis shows that Pdot-dye hybrid NPs are stable under large pH range, from pH 3.0 to pH 9.2. No aggregation was observed during proton diffusion experiment (Figure S7). To prove that fast pH probe signal change is due to rapid proton diffusion whether than leaking of fluorescence pH probe from Pdots, we compared UV-Vis absorption of Pdot-dye before and after the proton diffusion experiment and dialysis (dialyzing procedure see experimental part), no significant change was found, as shown in Figure S8.

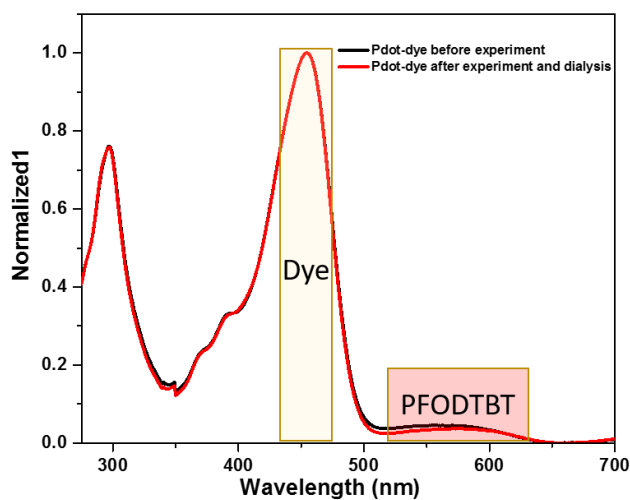


Figure S8. UV-Vis analysis of Pdot-dye before proton diffusion experiment (black line) and Pdot-dye after proton diffusion experiment and dialysis (red line).

2d. pH environment study under Photocatalysis process

pH environment in Pdots under photocatalysis process was then studied. In this study, pH environment (e.g. pH variation) instead of accurate pH determination was studied. Here, UV-Vis absorption of Pdot-dye was recorded, since maxima absorption shift at $\lambda = 455$ nm and $\lambda = 402$ nm is pH dependent, and absorption intensity ratio at $\lambda = 455$ nm and $\lambda = 402$ versus pH has same similar trend as fluoremetric measurement. Therefore, kinetic UV-vis absorption was recorded by using optic ocean under laser $\lambda = 535$ nm (within the absorption range of Pdots, out of the absorption wavelength of dye). Absorption was recorded per second, 30 min in total, laser was on at $t = 0$. Raw data as well as ratio of I_{455}/I_{402} are present in Figure S9. Preliminary results show a stable pH environment inside vesicle during photocatalysis process (as shown in Figure S9), indicating that a fast proton diffusion across polymer shell might contribute to this stable pH environment maintaining and the bulk solution continuously offers protons for proton reduction inside the Pdots as well as at the interface between Pdots and bulk solution. Kinetic study of photocatalytic hydrogen generation of Pdot-HTPS hybrid NPs was carried out using a Unisense microsensor, as shown in Figure S10a and b. An initial rate constant for hydrogen generation of 9.0 ± 0.1 mmol $g^{-1}h^{-1}$ was obtained with PFODTBT concentration of $0.9 \mu g ml^{-1}$, under light of $\lambda = 550$ nm (11.2 mW cm^{-2}). DLS analysis indicate stable Pdot-HTPS hybrid NPs after 100 min of light exposure (see Figure S10c).

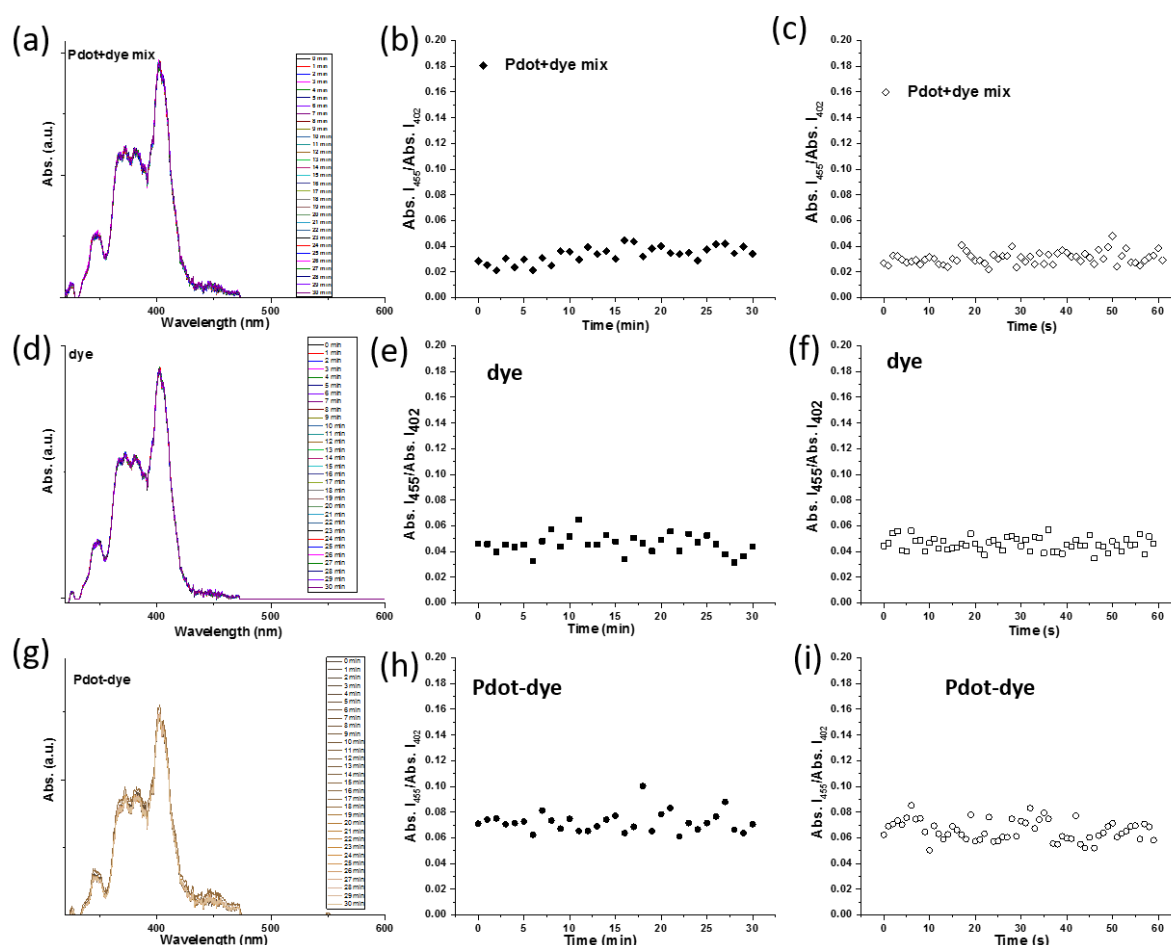


Figure S9. (a), (d) and (g) UV-Vis absorption of Pdot+dye mixture, dye and Pdot-dye, respectively; (b), (e) and (h) show absorption intensity ratio at $\lambda = 455$ nm and $\lambda = 402$ nm over 30 min; (c), (f) and (i) show absorption intensity ratio at $\lambda = 455$ nm and $\lambda = 402$ nm at the 8th min.

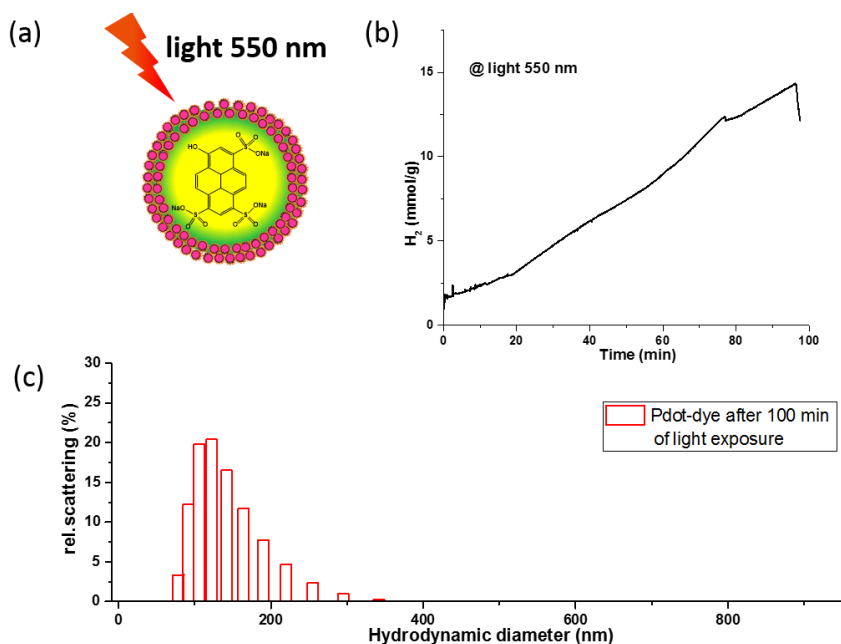


Figure S10. (a) Scheme of Pdot-dye colloid under light of $\lambda = 550$ nm, light intensity = 11.2 mV cm^{-2} ; (b) light at $\lambda = 550$ nm driven hydrogen generation. Condition: Pdot-dye NPs with PFODTBT $0.9 \mu\text{g mL}^{-1}$, 0.2 M ascorbic acid, pH 4; (c) DLS analysis of Pdot-dye after 100 min of light exposure.

3. Effect of Pdots size and hollow structure on photocatalysis

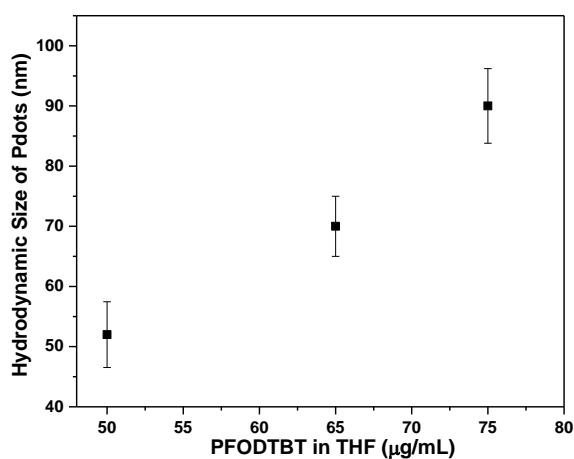


Figure S11. Final size of Pdots depend on initial PFODTBT concentration in THF.

Hollow Pdots with various size were prepared by varying the initial PFODTBT concentration in THF, MN = 50 nm, 70 nm, and 90 nm were obtained by tuning the concentration.

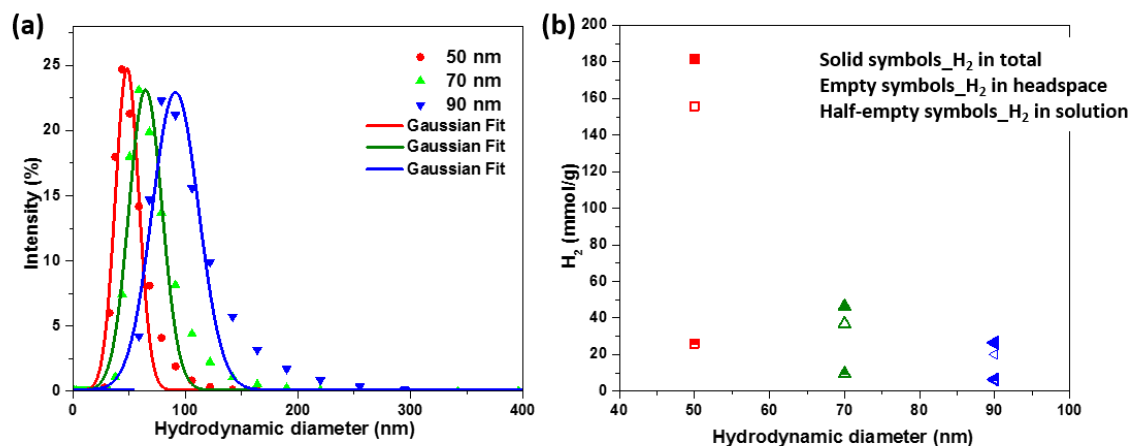


Figure S12. a) DLS analysis of hydrodynamic diameter of synthesized particles with average size of 50 nm, 70nm and 90 nm; b) kinetic record of hydrogen generation of Pdots with size of 50, 70 and 90 nm; b) semi-empty symbols indicate H₂ in solution, empty symbols indicate H₂ in headspace, solid symbols indicate total H₂ generation of Pdots with various size. Particle concentration for all particles size is at 23 $\mu\text{g mL}^{-1}$ (based on PFODTBT concentration), all data were recorded from cycle 0.

Considering low solubility of H₂ in aqueous, the final amount of H₂ in headspace was measured using gas chromatography (GC) (note: GC was measured after reaching equilibrium of H₂ between the solution and the headspace).

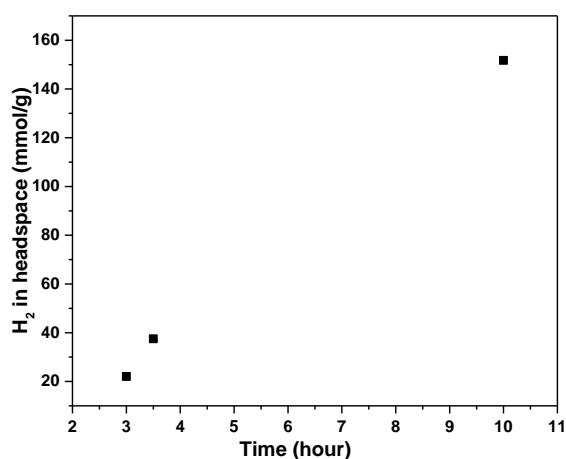


Figure S13. GC measurement of H₂ in headspace for Pdots with 50 nm at PFODTBT concentration 23 $\mu\text{g mL}^{-1}$, 0.2 M ascorbic acid, pH 4.

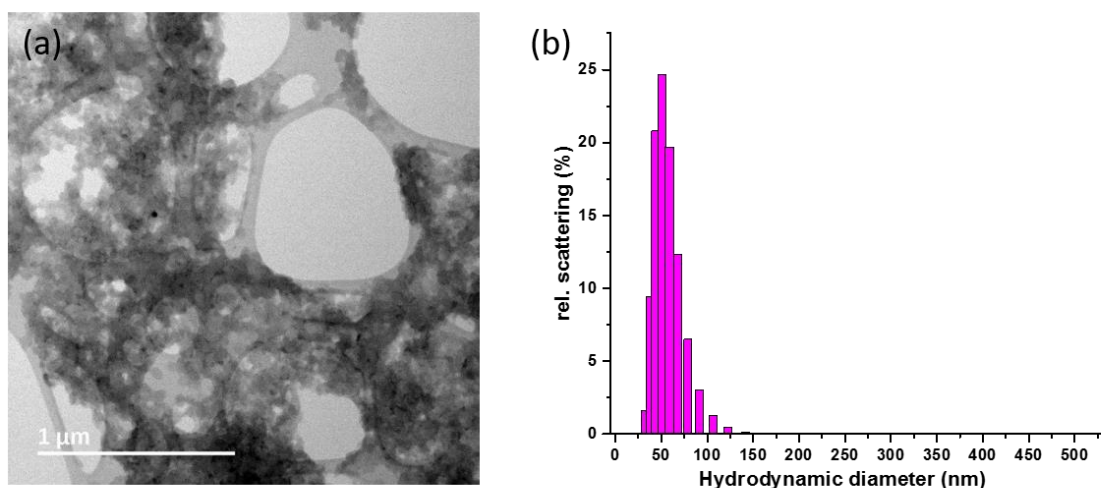


Figure S14. Pd dots with solid NPs prepared without sonication: (a) STEM analysis; (b) DLS analysis.

Pdots with 'solid' NPs are prepared as similar method as hollow particles without sonication, PFODTBT was dissolved in tetrahydrofuran (THF) at concentration of $50 \mu\text{g mL}^{-1}$, and PS-PEG-COOH in THF at concentration of 1.0 mg mL^{-1} . Then, add $100 \mu\text{L}$ of PS-PEG-COOH solution into 10 mL of PFODTBT solution under sonication (or magnetic stirring), leave the mixture for stirring for 0.5 hr. Then this mixture solution was add into 20 mL of distilled water drop-wisely with stirring, yielding a clear and dark red solution. Argon stripping was then carried out in order to remove THF. After completely remove THF, this colloidal solution was filtered through a $0.45 \mu\text{m}$ syringe filter before other analysis. STEM analysis show Pd dots with solid NPs (Figure S3a) with average hydrodynamic diameter of 50 nm (Figure S3b). NOTE: solid Pd dots NPs with same size were also obtained with slow THF evaporation without Ar stripping, means no effect of Ar stripping on nanoparticle morphology was found.

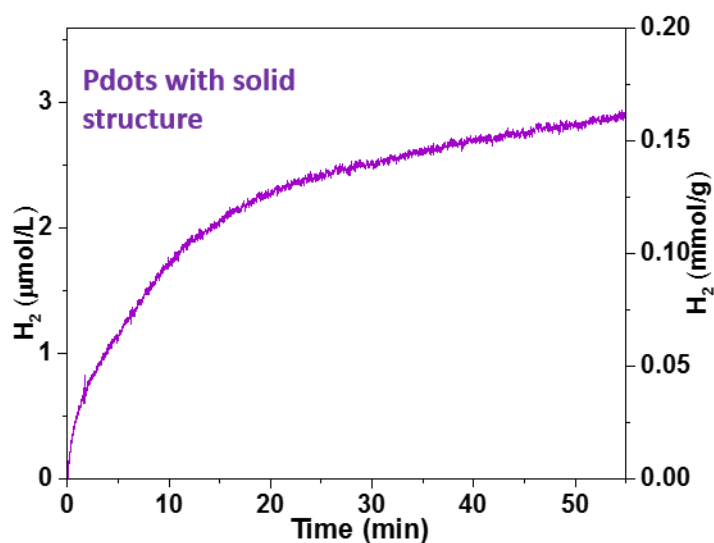


Figure S15. Kinetic hydrogen evolution study of Pdots with solid NPs

In a controlled experiment, photocatalytic of Pdots with solid NPs shows a much lower initial HER rate of $0.4 \text{ mmol g}^{-1}\text{h}^{-1}$, 50 times decrease in photocatalytic activity was observed compared to hollow Pdots. Hollow nanoparticles as photocatalysts have advantages in large light harvesting, high specific surface area and spatial anisotropic charge separation,⁶⁻¹⁰ which significantly enhanced photocatalytic activity of hollow structure. Plus, ultrasonic assisted self-assembly of conducting polymer has contribute to better organic photovoltaic cells performance than randomly aggregated polymer without sonication.¹¹ The self-assembly of conducting polymer along polymer shell with the assistant of ultra-sonication contribute to this highly enhanced HER rate.

4. Hydrogen generation analysis with polymer organic droplet (without removing of THF)

Both organic and aqueous solutions were stripped with Ar flow for 10 min to remove dissolved oxygen. After then PFODTBT with PS-PEG-COOH THF solution added in to water phase (contain 0.2 M ascorbic acid, pH4) quickly under stirring, after mixing, continue Ar flow for another 10 min in the headspace to remained air. A series of organic to aqueous volume ratios were studied and compared: organic to water = 1:0, 1:1, 1:3 and 1:7. The mixtures were than leave with under a LED PAR38 lamp. Hydrogen generation was analyzed by GC every 3 hrs, 10 hrs in total, however no hydrogen was found in all cases. The result again suggests that the structure of Pdots is really important for photocatalysis. With a hollow structures containing many channels, the protons can be efficiently reduced by reactive sites located in Pdots with such kind of architecture. Regarding the reactive sites, in our previous work, we experimentally proved that the benzothiadiazole (BT) units play important roles in photocatalysis. DFT

computation provides a hypothesis that the protons would interact with N atoms in BTs to get reduced in reduced Pdots. Recently, Kosco and co-workers reported that the residual Pd in F8BT (PFBT) Pdots indeed plays important role in photocatalysis⁴. In our prepared PDODTBT Pdots, there is 0.19 wt% of Pd detected by ICP measurement. So, Pd as a co-catalyst therefore should not be excluded in PDODTBT Pdots at this moment until further clarifying by solid evidences from more experiments. Overall our results show that the hollow structure of Pdots are important in high photocatalytic performance.

Reference

1. Bang, J. H.; Suslick, K. S., Applications of Ultrasound to the Synthesis of Nanostructured Materials. *Advanced Materials* **2010**, *22* (10), 1039-1059.
2. Suslick, K. S., Sonochemistry. *Science* **1990**, *247* (4949), 1439-1445.
3. Paxton, W. F.; Price, D.; Richardson, N. J., Hydroxide ion flux and pH-gradient driven ester hydrolysis in polymer vesicle reactors. *Soft Matter* **2013**, *9* (47), 11295-11302.
4. Weingarten, A. S.; Kazantsev, R. V.; Palmer, L. C.; McClendon, M.; Koltonow, A. R.; Samuel, A. P. S.; Kiebal, D. J.; Wasielewski, M. R.; Stupp, S. I., Self-assembling hydrogel scaffolds for photocatalytic hydrogen production. *Nature Chemistry* **2014**, *6*, 964.
5. Maassen, S. J.; van der Schoot, P.; Cornelissen, J. J. L. M., Experimental and Theoretical Determination of the pH inside the Confinement of a Virus-Like Particle. *Small* **2018**, *14* (36), 1802081.
6. Nguyen, C. C.; Vu, N. N.; Do, T.-O., Recent advances in the development of sunlight-driven hollow structure photocatalysts and their applications. *Journal of Materials Chemistry A* **2015**, *3* (36), 18345-18359.
7. Zhao, S.; Zhang, Y.; Fang, J.; Zhang, H.; Wang, Y.; Zhou, Y.; Chen, W.; Zhang, C., Self-Assembled Mesoporous Carbon Nitride with Tunable Texture for Enhanced Visible-Light Photocatalytic Hydrogen Evolution. *ACS Sustainable Chemistry & Engineering* **2018**, *6* (7), 8291-8299.
8. Sun, J.; Zhang, J.; Zhang, M.; Antonietti, M.; Fu, X.; Wang, X., Bioinspired hollow semiconductor nanospheres as photosynthetic nanoparticles. *Nature Communications* **2012**, *3*, 1139.
9. Zhao, Z.; Wang, X.; Shu, Z.; Zhou, J.; Li, T.; Wang, W.; Tan, Y., Facile preparation of hollow-nanosphere based mesoporous g-C₃N₄ for highly enhanced visible-light-driven photocatalytic hydrogen evolution. *Applied Surface Science* **2018**, *455*, 591-598.
10. Ghosh, S.; Kouamé, N. A.; Ramos, L.; Remita, S.; Dazzi, A.; Deniset-Besseau, A.; Beaunier, P.; Goubard, F.; Aubert, P.-H.; Remita, H., Conducting polymer nanostructures for photocatalysis under visible light. *Nature Materials* **2015**, *14*, 505.
11. Kim, B.-G.; Kim, M.-S.; Kim, J., Ultrasonic-Assisted Nanodimensional Self-Assembly of Poly-3-hexylthiophene for Organic Photovoltaic Cells. *ACS Nano* **2010**, *4* (4), 2160-2166.